Published in final edited form as:
Arch Gen Psychiatry. 2011 April ; 68(4): 340–350. doi:10.1001/archgenpsychiatry.2010.175.

Hippocampal interneurons in bipolar disorder

Christine Konradi, PhD[1,*], **Eric I. Zimmerman, BS**[2], **C. Kevin Yang, BS**[2], **Kathryn M. Lohmann, BS**[2], **Paul Gresch, PhD**[1], **Harry Pantazopoulos, ALM**[3], **Sabina Berretta, MD**[3,4], and **Stephan Heckers, MD**[2]

[1]Department of Pharmacology, Vanderbilt University, Nashville, TN, USA

[2]Department of Psychiatry, Vanderbilt University, Nashville, TN, USA

[3]Translational Neuroscience Laboratory, McLean Hospital, Belmont, MA, USA

[4]Department of Psychiatry, Harvard Medical School

Abstract

Context—Postmortem studies have reported decreased density and decreased gene expression of hippocampal interneurons in bipolar disorder, but neuroimaging studies of hippocampal volume and function have been inconclusive.

Objective—To assess hippocampal volume, neuron number and interneurons in the same specimens of bipolar and healthy control subjects.

Design—Whole human hippocampi of 14 bipolar and 18 healthy control subjects were cut at 2.5 mm intervals and sections from each tissue block were either Nissl-stained or stained with antibodies against somatostatin or parvalbumin. Messenger RNA was extracted from fixed tissue and real-time quantitative PCR was performed.

Setting—Basic research laboratories at Vanderbilt University and McLean Hospital.

Samples—Brain specimens from the Harvard Brain Tissue Resource Center at McLean Hospital.

Main Outcome Measures—Volume of pyramidal and non-pyramidal cell layers, overall neuron number and size, number of somatostatin- and parvalbumin-positive interneurons and messenger RNA levels of somatostatin, parvalbumin and glutamic acid decarboxylase 1.

Results—The two groups did not differ in the total number of hippocampal neurons, but the bipolar disorder group showed reduced volume of the non-pyramidal cell layers, reduced somal volume in cornu ammonis sector 2/3, reduced number of somatostatin and parvalbumin-positive neurons, and reduced messenger RNA levels for somatostatin, parvalbumin and glutamate decarboxylase 1.

Conclusions—Our results indicate a specific alteration of hippocampal interneurons in bipolar disorder, likely resulting in hippocampal dysfunction.

[*]Correspondence: Christine Konradi, PhD, Vanderbilt University, MRB 3, Room 8160A; 465 21st Avenue South, Nashville TN 37232-8548; Phone: 615-936-1021; christine.konradi@vanderbilt.edu.

Financial Disclosure: The authors have no relevant financial interest in this manuscript.

Christine Konradi had full access to all of the data in the study and takes responsibility for the integrity of the data and the accuracy of the data analysis

Introduction

Bipolar disorder affects about 2.6 percent of the U.S. population[1] and is one of the leading causes of disability[2]. Despite it's health impact, bipolar disorder is relatively understudied. Publications indexed in PubMed since 1980 with the term "schizophrenia" outweigh those with the term "bipolar disorder" by 8:1. This bias can be traced back to Emil Kraepelin's strong hypothesis that schizophrenia is a structural brain disorder, whereas bipolar disorder has no neural substrate[3].

Genetic, neuroimaging and postmortem studies are now challenging Kraepelin's dichotomy[4]. Abnormalities of the limbic system are particularly compelling as neural substrates for the main features of bipolar disorder, such as depression, mania, psychosis and cognitive deficits[5–7]. However, the emerging literature on the hippocampus in bipolar disorder has been inconclusive. Neuroimaging studies have reported increases, decreases or no changes of hippocampal volume in bipolar disorder[6–11]. Neuropsychological studies have demonstrated significant impairment of declarative memory in bipolar disorder[12, 13], but this deficit has not been linked consistently to abnormalities of the hippocampus[7, 14, 15].

In contrast, post-mortem studies have provided compelling evidence for abnormalities of the hippocampus in bipolar disorder. The initial finding of decreased non-pyramidal neuron density[16] was confirmed and extended by an in-situ hybridization study that revealed decreased expression of glutamic acid decarboxylase 1 (GAD1) mRNA, coding for the enzyme that synthesizes GABA (gamma-aminobutyric acid)[17]. Furthermore, the expression of mRNAs coding for proteins expressed in subsets of hippocampal neurons was decreased in bipolar disorder[18, 19]. In concordance, abnormalities of gene networks can be linked to distinct mechanisms of interneuron dysfunction in schizophrenia and bipolar disorder[20–22]. Taken together, the evidence for GABAergic dysfunction in bipolar disorder is compelling[23, 24], though the structural correlates are still elusive.

In each of the four cornu ammonis sectors (CA 1–4) of the hippocampus, GABAergic interneurons are interspersed with a much larger number of glutamatergic principal neurons. The ratio of glutamatergic to GABAergic neurons in the human hippocampus is in excess of 10:1[16, 25], but a single interneuron provides inhibition through 1,000 to 2,000 synapses with principal neurons[26, 27]. Interneurons of the human hippocampus are crucial for the tonic and phasic inhibition of neighboring neurons, giving rise to characteristic electrical rhythms that are essential for cognitive processing[28–30].

Here we used an unbiased stereological approach to determine overall neuron number and neuron size in whole hippocampal specimens. Furthermore, we measured the volume of pyramidal and non-pyramidal cell layers and we counted specific populations of GABAergic interneurons.

Hippocampal GABAergic neurons are classified based on the expression of calcium-binding proteins such as parvalbumin, calbindin and calretinin, and of neuromodulators such as somatostatin, neuropeptide Y, vasoactive intestinal peptide and nitric oxide synthase[26, 31]. These 'markers' identify subtypes of hippocampal interneurons with distinct morphological, physiological and molecular properties[27]. We used whole hippocampal specimens to estimate the number of interneurons expressing somatostatin and parvalbumin. Somatostatin-releasing neurons make up 30% to 50% of all hippocampal interneurons[32]. They control the efficacy and plasticity of excitatory inputs to principal neurons[26] and can modulate seizure activity[33]. Neurons expressing the calcium-binding protein parvalbumin play a key role in the generation of gamma oscillations[34], which are abnormal in patients with cognitive impairments and psychiatric disorders[35].

We show here that, in the context of normal total hippocampal neuron number, the number of somatostatin-positive and parvalbumin-positive hippocampal interneurons was markedly reduced in bipolar disorder. This finding was validated by the study of mRNA expression, using a novel real-time quantitative PCR approach for fixed human brain tissue. Furthermore, the volume of the non-pyramidal cell layer was reduced, as was the cell body volume in sectors CA2/3.

Methods

Sample

Brains were collected at the Harvard Brain Tissue Resource Center (HBTRC; McLean Hospital, Belmont, MA). The HBTRC is funded by NIH and follows all regulations implemented by the Office for Human Research Protections.

For all the subjects included in this study, two psychiatrists established DSM-IV diagnoses based on the review of a questionnaire filled out by legal next of kin and a review of all available medical records. Control cases had sufficient information from next of kin and medical records to rule out major medical, neurologic, and psychiatric conditions. All brains underwent a neuropathological exam and cases with histopathological abnormalities were excluded from this study.

Two diagnostic groups, comprised of 18 normal control and 14 bipolar disorder subjects, were matched for gender, age, post-mortem interval, and hemisphere (Table 1). The sample included 14 matched pairs, which were chosen for the real-time, quantitative PCR (Q-PCR) experiments (Table 1). Samples of the present study were newly collected and did not overlap with samples used in a previous study[17].

Tissue collection and processing

The entire hippocampus was dissected from one hemisphere of each case. Tissue was immersion-fixed in 4.0% paraformaldehyde (0.1 M phosphate buffer (PBS), pH 7.4) at 4.0º C for 3 weeks. Hippocampi were placed in cryoprotectant (0.1 M PBS, pH 7.4/ 0.1% sodium azide/ 30.0% ethylene glycol/ 30.0% glycerol), immersed in agar and cut into 2.5 mm thick coronal slabs using an antithetic tissue slicer. Sections were cut from the top-most portion of each slab using a sliding microtome (American Optical Company, Buffalo, NY), with a thickness of 100 μm for Nissl-stain, or 50 μm for immunocytochemistry. Sections were mounted on gelatin-coated glass slides and stained with 0.1% cresyl violet (Nissl stain) or used for immunocytochemistry.

Immunocytochemistry

The immunocytochemical procedure was performed as described previously[36]. For both immunocytochemical experiments, all sections were processed simultaneously to avoid procedural differences. Each staining dish contained sections from bipolar and normal control subjects and all dishes were treated for the same duration (see supplement for details of the procedure).

The somatostatin antibody was diluted 1:500 (monoclonal rat anti synthetic cyclic somatostatin peptide corresponding to amino acids 1–14; Cat # MAB354, Millipore, Billerica, MA); the parvalbumin antibody was diluted 1:10,000 (monoclonal mouse anti frog muscle parvalbumin, clone PARV-19; Cat #P3088, Sigma). Secondary antibodies were biotinylated, goat anti-rat IgG for somatostatin, and goat anti-mouse IgG for parvalbumin (Vector laboratories). Secondary antibodies were diluted 1:500.

Morphometric analysis

All cases were coded and data collection was completed without knowledge of diagnostic group. Morphometric analysis was performed using a Zeiss Axioskop 2 Plus microscope (Germany) equipped with a LEP MAC 5000 automated stage (Ludl Electronic Products, Hawthorne, NY). The microscope was interfaced with the Stereo Investigator stereological software (v 6.55, Microbrightfield, Colchester, VT) via an Optronics DEI-750 video camera (Goleta, CA). For the analysis of total neuron number and somal volume, we identified one pyramidal cell layer in three sectors (CA1, CA2/3 and CA4) and two non-pyramidal cell layers in sectors CA 1 and CA2/3 (Figure 1, see supplement for details). For the analysis of somatostatin- and parvalbumin-positive neurons, we delineated three hippocampal sectors (CA1, CA2/3 and CA4) without further separation into layers (Figure 2, see supplement for details).

Volume and total neuron number estimates

Uniformly random sampling of CA neurons was conducted in the pyramidal cell layer throughout the entire hippocampal formation. Sections were sampled at a fixed interval of 2.5 mm with a random starting point in the coronal plane (average of 17 sections per hippocampus). Volume estimates of layers in the CA sectors were calculated from the product of known intervals between sections and contour measurements. Weighted means for section thicknesses were determined at every sampling site by differential focusing using a 100X oil-immersion objective (Zeiss, Plan-Apochromat, NA 1.40). The vertical movement of the stage was determined by a microcator (Heidenhain, Germany).

The optical fractionator method was used to obtain an unbiased estimate of total neuron number in each of the CA sectors. The optical fractionator approach is independent of volume measurements and is unaffected by tissue shrinkage in the z axis[37, 38]. Neurons were counted within a three-dimensional dissector box (50 × 50 × 10 μm). Dissector counting frames were positioned in a systematically random fashion in each CA sector (1200 × 1200 μm for CA1 and 600 × 600 μm for CA2/3 and CA4). Neurons were counted only when their associated nucleoli were in focus within the dissector box and not touching the left or bottom side of the dissector box[39]. In order to avoid the issues of lost caps and other cutting artifacts, a 2 μm guard-zone was applied to the top and bottom of each section[39]. This stereological sampling protocol resulted in the following average cell count (Q), counting sites (F) and average estimated volume coefficents of errors (CE): CA1 = 284/131/0.06 (Q/F/CE); CA2/3 = 242/104/0.07; CA4 = 144/116/0.09.

The estimate of total neuron number (N) per CA sector was calculated as the product of the number of neurons counted within the dissector box (ΣQ-) and the reciprocal of the fraction of the CA sector sampled[40]. The reciprocal fraction is the product of the fraction of the sections sampled, the fraction of the area of the sections sampled, and the fraction of the section thickness sampled. This last fraction is given as the ratio of dissector box height to number-weighted mean section thickness, which is calculated from the local section thickness and local neuron count in the i'th counting frame. This estimation allows thickness calculations to be unbiased even if homogenous, non-uniform deformation in the z-axis occurs[37, 38] (average section thickness in our samples: CA1, 20.45 μm; CA2/3, 19.69 μm; CA4, 19.25 μm.)

Somal volume estimates

The nucleator method[41, 42] was used to estimate somal volume of neurons in each of the CA sectors. The nucleator probe superimposed four isotropic rays emanating from the nucleolus of each sampled neuron. Estimates of area and volume were calculated from the recorded distance between nucleolus and cell wall for each ray. Neurons were sampled from sections

at 7.5 mm intervals. The counting frame dimensions were 2500 × 2500 μm for the CA1 sector and 1000 × 1000 μm for the CA2/3 and CA4 sectors. This resulted in the following average cell count (Q), counting sites (F) and estimated volume CE per sector: CA1 = 54.8/17.1/0.01 (Q/F/CE); CA2/3 = 57.7/14.2/0.01; CA4 = 41.8/15.4/0.02.

Total immunopositive neuron estimates

The somatostatin- and parvalbumin-positive neurons were assessed in sections of 5 mm intervals. First, volume estimates of the three CA sectors were calculated from the product of known intervals between sections and contour measurements. Second, using the automated stage of the microscope, each section was systematically scanned through the full x, y, and z axes using a 40× objective to count each parvalbumin- and somatostatin-labeled element with a cell body and at least one process clearly identifiable within each of the three CA sectors (see Figure 2). The average regional CE was 0.02 (CA1 and CA4) and 0.03 (CA2/3). Third, the total number of somatostatin- and parvalbumin-positive neurons was calculated as total number of cells counted/50 μm * 5000 μm.

Real-time quantitative PCR (Q-PCR)

Three hippocampal sectors (CA 1, 2/3 and 4) were dissected from a 2.5 mm slab of fixed, frozen tissue, collected from the middle body of the hippocampus, and RNA was extracted using the Recoverall Total Nucleic Acid Isolation kit (Applied Biosystems, Foster City, CA, USA). Cornu ammonis borders were determined on an adjacent, cresyl violet-stained slice. The tissue was digested with protease, RNA isolated onto a glass filter, washed, and eluted with water. Samples were vacuum-dried and re-suspended in a volume of 20 μl water. RNA quantity was measured using the NanoDrop 1000A Spectrophotometer, with A260/A280 ratios ranging from 1.8–2.1.

One μg RNA was reversed transcribed into cDNA using the High-Capacity cDNA Reverse Transcription Kit (Applied Biosystems, Foster City, CA, USA). Reverse transcription was performed in an Eppendorf Mastercycler (Hamburg, Germany) for 10 min at 25°C, 120 min at 37°C, and 5 sec at 85°C. The Taqman PreAmp Master Mix Kit (Applied Biosystems) was used to increase the quantity of specific cDNA targets for qPCR analysis. For the preamplification reaction, the primers and probes of five Taqman assays (SST, PVALB, GAD1, ACTB and FLNA) were pooled together, with 1X Tris–EDTA (TE) buffer. The preamplification reaction was performed in 50 μl reactions containing 25 μl of TaqMan PreAmp master mix, 12.5 μl of the pooled assay mix, 10 μl of cDNA sample and 2.5 μl of nuclease-free water. Cycling conditions were 10 min at 95°C, 14 cycles of 15 s at 95°C and 4 min at 60°C using an Eppendorf Mastercycler (Hamburg, Germany).

The preamplified products were diluted 1:20 using TE buffer. The gene expression reaction was performed in 20 μl reactions containing 10 μl of TaqMan gene expression master mix, 5 μl of diluted preamp product, 1 μL of TaqMan gene expression assay and 4 μL of nuclease-free water (Applied Biosystems). A standard curve was generated using five 1:5 dilutions of pooled preamplified products. The logarithm of the dilution value was plotted against the cycle threshold value. Each dilution curve contained blanks to control for cross-contamination. Dilution curves and blanks were run in duplicate and samples were run in triplicate. The following thermal cycling specifications were performed on the Stratagene Mx3005P instrument (Stratagene): 2 min at 50°C, 10 min at 95°C and 40 cycles each for 15 s at 95°C and 1 min at 60°C (reading temperature). The Stratagene MxPro QPCR software used the cycle threshold data from the standards to quantify the cDNAs for subject samples. Gene expression was normalized to β-actin and the actin binding protein filamin A, the latter of which has been shown to have equal expression levels in the hippocampus in bipolar disorder and controls[18]. Within each experiment, 96 data points could be collected, with 12

data points used for standard curves and blanks. Thus, for each sector 28 samples were examined in triplicates, and matched bipolar disorder - control subject pairs were used (Table 1).

Effect of treatment on somatostatin, parvalbumin and GAD1 mRNA levels

Male Sprague-Dawley rats (200 – 250 g at start of treatment) were treated chronically with either lithium, valproic acid, clozapine or haloperidol and hippocampi subjected to gene expression analysis. Supplemental table 1 shows treatment durations, subject numbers, route of administration, types of gene arrays used and mRNA levels of somatostatin, parvalbumin and GAD1.

Statistical analysis

Histological data were analyzed for subjects used in the Q-PCR analysis (n=14 per diagnostic group) and in the complete data set (n=14 bipolar disorder, n=18 controls; Table 1). We did not observe any significant difference between these two analyses and are reporting here the analysis of the complete data set. Hippocampal sectors were treated as repeated measures. To reduce the weight of outliers, all histological data were log2 transformed for analysis. Initially, multivariate analysis of covariance (MANCOVA) was performed with ‘diagnosis’ as the between-subject effect and ‘CA sector’ as the within-subject effect. Covariates included gender, age, postmortem interval (PMI) and hemisphere, as indicated in the results section. In case of a significant diagnosis effect in the MANCOVA model, we tested for group differences in individual CA sectors using Student’s t- test and Cohen’s d effect size calculation. Due to the 96-well limitation in Q-PCR experiments samples had to be grouped into CA sectors and each CA sector was independently analyzed. The JMP program (v 7.02) was used for all analyses.

Results

Hippocampal volume, cell number and cell volume

We studied volume and cell number in systematically sampled coronal sections of whole hippocampal specimens. In each section, we differentiated up to three sectors (CA1, 2/3 and 4) and three layers (stratum oriens, stratum pyramidale, stratum radiatum / lacunosum / moleculare (RLM) (Figure 1A). While hippocampal volume is a biased estimate due to postmortem tissue shrinkage, the ratio of pyramidal to non-pyramidal cell layer volumes is not. We found similar volumes of the CA1–4 pyramidal cell layer in the two groups, but the volume of the CA1–3 non-pyramidal cell layers was significantly smaller in bipolar disorder (main effect of diagnosis: $F [5,26]=5.57$, $p<=0.026$ with age, gender, hemisphere and PMI as covariates; Cohen’s $d=0.84$) (Figure 1B).

The average total number of neurons in pyramidal layers CA 1–4 was 10,877,208 ± 386,524 (average ± SEM), with the largest number in CA1 (8,228,372 ± 303,270) and significantly fewer numbers in CA 2/3 (1,665,760 ± 84,561) and CA 4 (983,077 ± 43,972) (main effect of sector: $F [2,25]=7.7$, $p<=0.002$ with age, gender, hemisphere and PMI as covariates). This pattern did not differ significantly between the two groups (main effect of diagnosis $F [1,26] = 0.8$, $p<=0.369$ with age, gender, hemisphere and PMI as covariates) (Figure 1C).

Average cell volume was similar across the three sectors (main effect of sector: $F [2,25]= 1.4$, $p<=0.267$; diagnosis, age, gender, hemisphere and PMI as covariates) and across the two groups (main effect of diagnosis $F [1,26]=2.8$, $p<=0.104$ with age, gender, hemisphere and PMI as covariates). However, a significant interaction was observed between diagnosis and sector ($F [2,25]=3.7$, $p<=0.04$ with age, gender, hemisphere and PMI as covariates), due

to significantly smaller cell volume of CA2/3 neurons in bipolar disorder (t [1,30]=−2.34, p<=0.026, Cohen's d=0.82) (Figure 1D).

Somatostatin- and parvalbumin-positive interneurons

We estimated the total number of somatostatin- and parvalbumin-positive hippocampal interneurons in sections adjacent to the Nissl-stained sections reviewed above. Somatostatin-positive neurons were small neurons with sparse labeling of the axon and dendritic tree and were found in pyramidal and non-pyramidal cell layers of sectors CA1–4 (Figure 2 A, C, E). Parvalbumin-positive neurons were larger neurons with extensive labeling of both axon and the dendritic tree and were found almost exclusively in the pyramidal cell layer (Figure 2 B, D, F).

The total number of somatostatin-positive neurons was largest in CA1 and smallest in CA2/3. This pattern was similar in both groups, but the total number of somatostatin-positive neurons was significantly reduced in bipolar subjects (F [1,26]=8.7, p<=0.007 with age, gender, hemisphere and PMI as covariates) (Figure 2 G). Sector CA1 (t [1,30]=−2.28, p<=0.030, Cohen's d=0.82) reached significance in a post-hoc analysis.

The total number of parvalbumin-positive neurons was largest in CA1 and smallest in CA4. This pattern was similar in both groups, but the total number of parvalbumin-positive neurons was significantly reduced in bipolar subjects (F [1,24]=5.4, p<=0.029; with age, gender, hemisphere and PMI as covariates) (Figure 2 H). Sectors CA1 (t [1,28]=−2.28, p<=0.031, Cohen's d=0.83) and CA4 (t [1,28]=−2.27, p<=0.031, Cohen's d=0.84) reached significance in a post-hoc t-test.

Gene expression levels of hippocampal interneurons

We studied hippocampal mRNA expression levels of somatostatin, parvalbumin and GAD1 in a subsample of the cases reviewed above (Table 1). Normalized mRNA expression levels of somatostatin were significantly lower in bipolar disorder (Figure 3). Differences in sectors CA1 (t[1,24]=−2.29, p<=0.031, Cohen's d=0.90), CA2/3 (t [1,24]=−2.5, p<=0.019, Cohen's d=0.98), and CA4 (t [1,24]=−2.1, p<=0.046, Cohen's d=0.83) reached significance. Normalized mRNA expression levels of parvalbumin were also significantly lower in bipolar disorder (Figure 3). Differences in sectors CA2/3 (t [1,24]=−2.38, p<=0.026, Cohen's d=0.93) and CA4 (F [1,24]=−2.94, p<=0.007, Cohen's d=1.15) reached significance. Finally, normalized GAD1 mRNA levels were significantly reduced in CA2/3 (t [1,24]=−2.2, p<=0.037, Cohen's d=0.864).

Effect of treatment

mRNA analysis of groups of rats treated with lithium carbonate, valproic acid or antipsychotic drugs did not show any effect of treatment on levels of somatoatatin, parvalbumin or GAD1 (supplemental table).

Comment

This study, using unbiased cell counting, immunocytochemistry and real-time quantitative PCR in the same specimens, provides strong evidence for a marked reduction of somatostatin- and parvalbumin-positive interneurons in bipolar disorder. While the number of these two subtypes of hippocampal interneurons was significantly reduced, total neuron number and the volume of the pyramidal cell layer were not different from the healthy control group. This confirms and considerably extends previous studies of hippocampal interneurons in bipolar disorder[16, 17].

Neuroimaging studies have reported conflicting results regarding hippocampal volume in bipolar disorder, in contrast to the overwhelming evidence for smaller hippocampal volume in schizophrenia[43] and depression[7]. Several recent meta-analyses have now concluded that overall hippocampal volume is not abnormal in bipolar disorder[10, 11, 44, 45]. Our finding of significantly reduced non-pyramidal (but normal pyramidal) cell layer volume in bipolar disorder provides compelling evidence for a subtle volume difference of the hippocampus, beyond the resolution of current imaging studies. The major components of the non-pyramidal cell layers in the human hippocampus are axonal projections (primarily from neurons within the hippocampus) and a variety of interneurons, including their extensive dendritic arborization[26, 27, 46]. It is unlikely that the axons of projection neurons are markedly abnormal in bipolar disorder, since total cell number and regional volume of the pyramidal cell layer were normal. However, the number of immuno-positive interneurons was reduced, which likely reduces their rich dendritic arborization, primarily in stratum RLM. Therefore, we interpret the pattern of volume change observed in the bipolar disorder subjects as further support for hippocampal interneuron pathology in bipolar disorder. New structural imaging protocols are now approaching the resolution necessary to indentify the pyramidal and non-pyramidal cell layers in the CA sectors of the human hippocampus[47–50]. Future neuroimaging studies should test for a layer-specific reduction of hippocampal volume in bipolar disorder.

Previous anatomical studies had demonstrated reduced density of hippocampal interneurons[16] and reduced expression of GAD1 mRNA[17] in bipolar disorder. However, it was not known whether this pattern was part and parcel of an overall reduced neuron number. It was also not clear which subtypes of hippocampal interneurons are affected in bipolar disorder. Our study clarifies the existing literature since it provides strong evidence that the reduced number of two, functionally important hippocampal interneurons is not in the context of an overall loss of hippocampal neurons in bipolar disorder. This has implications for several types of hippocampal information processing in bipolar disorder, which we briefly outline here.

Hippocampal interneurons modulate the activity of the principal (i.e., glutamatergic) hippocampal neurons, resulting in an increased signal-to-noise ratio and synchronized network activity. Fast oscillations in the gamma range (30–100Hz) provide an organized pattern for the temporal encoding of new information and the storage and recall of previously stored information[51–53]. Parvalbumin-expressing interneurons are crucial for the generation of gamma oscillations[34]. A reduction of parvalbumin-positive neurons leads to a loss of perisomatic inhibition of pyramidal neurons, which in turn affects network synchronization and memory formation[34, 35]. Previous studies have provided compelling evidence that several neuropsychiatric disorders, including schizophrenia, are characterized by disrupted gamma oscillation[54–56]. Our findings provide compelling evidence that a similar pattern of dysfunction is also present in bipolar disorder.

Between 30% to 50% of all interneurons in the hippocampus contain the neuromodulator somatostatin[32]. Somatostatin-positive interneurons ameliorate perturbations in glutamatergic neurotransmission, which has been found to be abnormal in affective disorders[57, 58]. These neurons regulate the efficacy and plasticity of excitatory inputs to principal neurons[26] and play an important role in the control of seizure activity[33]. Our finding of reduced somatostatin-positive hippocampal interneurons suggests that hippocampal disinhibiton is a feature of bipolar disorder and that interneurons are a potential site of action for anticonvulsants, a class of drugs with proven benefit in the treatment of bipolar disorder, particularly mania[59].

We can only speculate about the behavioral implication of reduced hippocampal interneuron number in bipolar disorder. On the one hand, reciprocal connections of the posterior hippocampus ensure that the constructive process of memory encoding and retrieval creates accurate representations of experience[60, 61]. On the other hand, projections to and from the anterior hippocampus regulate affective processes[62]. It is likely that impairments in these hippocampal functions[63, 64] lead to poor functional outcomes in bipolar disorder patients[13, 65].

We did observe a significant decrease in the size of hippocampal neurons, most pronounced in sector CA2/3, in line with a similar report of decreased pyramidal cell size in CA1 in bipolar disorder[66]. The somal size of adult hippocampal neurons could be a distal read-out of neurodevelopmental abnormalities or a more proximal consequence of malfunction of trophic factors and synaptic remodeling during adulthood. Risk genes associated with psychotic disorders, including DISC1 and neuregulin have been associated with regulation of neuronal size[67, 68]. Somal size remains plastic during adulthood and the known change of hippocampal volume during lithium treatment[69, 70] could be mediated through changes in neuronal size. Concurrently, the normal decrease of somal size during adulthood could be accelerated in bipolar disorder, explaining the hippocampal volume reduction found in some adult bipolar disorder samples[71].

Our study design does have limitations. First, the sample size is small, in large part due to the fact that whole hippocampal specimens are difficult to obtain. However, the effect sizes of the total somatostatin- and parvalbumin-positive neuron number reduction were reassuringly large. Second, it is not clear whether our findings in a severely ill group of psychotic bipolar disorder subjects can be generalized to the larger group of bipolar disorder subjects. The majority of patients in our study were diagnosed retrospectively with DSM-IV-TR Bipolar Disorder, Type I, with psychotic features. The average age of onset was 23 years and average duration of illness was 28 years. For 8 of the 14 bipolar disorder subjects we could identify a first-degree relative with an affective or non-affective psychotic disorder.

Third, the immuno-positive neurons were not studied with the fractionator or dissector and the sampling regions differed between the Nissl and immunocytochemical stains. This is similar to previous studies[36, 72] and was due to the requirement to have consistent and reliable criteria for the demarcation of the reference volume and the objects to be sampled. Fourth, the total number estimates of the somatostatin- and parvalbumin-positive neuron number in the human hippocampus are affected by several confounding post-mortem effects[73] and may be an underestimate[26, 74]. However, there is no reason to assume that this potential bias is limited to the bipolar disorder group only. Finally, effects of treatment cannot be ruled out, though we examined mRNA levels of somatostatin, parvalbumin and GAD1 in rat hippocampi and could not find any effect of drugs commonly prescribed in bipolar disorder.

Our study contributes to the evolving nosology of psychotic disorders. There is now compelling evidence for shared genetic mechanisms of both psychotic bipolar disorder and schizophrenia[4, 75]. Our results confirm and extend previous findings of hippocampal interneuron pathology in both affective and non-affective psychosis[19, 22]. This will lead to novel models of disease mechanism beyond the Kraepelinian dichotomy[76, 77].

In conclusion, we present strong evidence for significant abnormalities of hippocampal interneurons in bipolar disorder, Type I. These findings have major implications for models of information processing in bipolar disorder and provide a rationale for the efficacy of

existing[78], and the development of novel, pharmacological interventions of this major psychiatric disorder.

Supplementary Material

Refer to Web version on PubMed Central for supplementary material.

Acknowledgments

Funding/Support: This work was supported by the National Institute of Mental Health [MH67999 (SH), MH74000 (CK) and MH068855 (Dr. Benes, HBTRC)]. The content is solely the responsibility of the authors and does not necessarily represent the official views of the funding institute or the National Institutes of Health.

References

1. Kessler RC, Chiu WT, Demler O, Merikangas KR, Walters EE. Prevalence, severity, and comorbidity of 12-month DSM-IV disorders in the National Comorbidity Survey Replication. Arch Gen Psychiatry. 2005 Jun; 62(6):617–627. [PubMed: 15939839]
2. Lopez, AD.; Mathers, CD.; Ezzati, M.; Jamison, DT.; Murray, CJL. Global Burden of Disease and Risk Factors. Washington, DC: World Bank and Oxford University Press; 2006.
3. Kraepelin, E. Psychiatrie. Ein Lehrbuch für Studierende und Ärzte. Achte, vollständig umgearbeitete Auflage. 3. Band. Klinische Psychiatrie. 2. Teil. Leipzig: Verlag von Johann Ambrosius Barth; 1913.
4. Craddock N, Owen MJ. Rethinking psychosis: the disadvantages of a dichotomous classification now outweigh the advantages. World Psychiatry. 2007 Jun; 6(2):84–91. [PubMed: 18235858]
5. Phillips ML. The neural basis of mood dysregulation in bipolar disorder. Cogn Neuropsychiatry. 2006 May; 11(3):233–249. [PubMed: 17354070]
6. Brambilla P, Hatch JP, Soares JC. Limbic changes identified by imaging in bipolar patients. Curr Psychiatry Rep. 2008 Dec; 10(6):505–509. [PubMed: 18980734]
7. Savitz J, Drevets WC. Bipolar and major depressive disorder: neuroimaging the developmental-degenerative divide. Neurosci Biobehav Rev. 2009 May; 33(5):699–771. [PubMed: 19428491]
8. Keener MT, Phillips ML. Neuroimaging in bipolar disorder: a critical review of current findings. Curr Psychiatry Rep. 2007 Dec; 9(6):512–520. [PubMed: 18221633]
9. Konarski JZ, McIntyre RS, Kennedy SH, Rafi-Tari S, Soczynska JK, Ketter TA. Volumetric neuroimaging investigations in mood disorders: bipolar disorder versus major depressive disorder. Bipolar Disord. 2008 Feb; 10(1):1–37. [PubMed: 18199239]
10. Bora E, Fornito A, Yucel M, Pantelis C. Voxelwise meta-analysis of gray matter abnormalities in bipolar disorder. Biol Psychiatry. 2010 Mar 17; 67(11):1097–1105. [PubMed: 20303066]
11. Ellison-Wright I, Bullmore E. Anatomy of bipolar disorder and schizophrenia: a meta-analysis. Schizophr Res. 2010 Mar; 117(1):1–12. [PubMed: 20071149]
12. Robinson LJ, Ferrier IN. Evolution of cognitive impairment in bipolar disorder: a systematic review of cross-sectional evidence. Bipolar Disord. 2006 Apr; 8(2):103–116. [PubMed: 16542180]
13. Bora E, Yucel M, Pantelis C. Neurocognitive markers of psychosis in bipolar disorder: A meta-analytic study. J Affect Disord. 2010 Mar 13.
14. Frey BN, Andreazza AC, Nery FG, et al. The role of hippocampus in the pathophysiology of bipolar disorder. Behav Pharmacol. 2007 Sep; 18(5–6):419–430. [PubMed: 17762510]
15. Hall J, Whalley HC, Marwick K, et al. Hippocampal function in schizophrenia and bipolar disorder. Psychol Med. 2010 May; 40(5):761–770. [PubMed: 19732478]
16. Benes FM, Kwok EW, Vincent SL, Todtenkopf MS. A reduction of nonpyramidal cells in sector CA2 of schizophrenics and manic depressives. Biol Psychiatry. 1998 Jul 15; 44(2):88–97. [PubMed: 9646890]
17. Heckers S, Stone D, Walsh J, Shick J, Koul P, Benes FM. Differential hippocampal expression of glutamic acid decarboxylase 65 and 67 messenger RNA in bipolar disorder and schizophrenia. Arch Gen Psychiatry. 2002 Jun; 59(6):521–529. [PubMed: 12044194]

18. Konradi C, Eaton M, MacDonald ML, Walsh J, Benes FM, Heckers S. Molecular evidence for mitochondrial dysfunction in bipolar disorder. Arch Gen Psychiatry. 2004 Mar; 61(3):300–308. [PubMed: 14993118]
19. Knable MB, Barci BM, Webster MJ, Meador-Woodruff J, Torrey EF. Molecular abnormalities of the hippocampus in severe psychiatric illness: postmortem findings from the Stanley Neuropathology Consortium. Mol Psychiatry. 2004 Jun; 9(6):609–620. 544. [PubMed: 14708030]
20. Benes FM, Lim B, Matzilevich D, Walsh JP, Subburaju S, Minns M. Regulation of the GABA cell phenotype in hippocampus of schizophrenics and bipolars. Proc Natl Acad Sci U S A. 2007 Jun 12; 104(24):10164–10169. [PubMed: 17553960]
21. Benes FM, Lim B, Subburaju S. Site-specific regulation of cell cycle and DNA repair in post-mitotic GABA cells in schizophrenic versus bipolars. Proc Natl Acad Sci U S A. 2009 Jul 14; 106(28):11731–11736. [PubMed: 19564623]
22. Benes FM. Relationship of GAD(67) regulation to cell cycle and DNA repair in GABA neurons in the adult hippocampus: bipolar disorder versus schizophrenia. Cell Cycle. 2010 Feb; 9(4):625–627. [PubMed: 20107308]
23. Brambilla P, Perez J, Barale F, Schettini G, Soares JC. GABAergic dysfunction in mood disorders. Mol Psychiatry. 2003 Aug; 8(8):721–737. 715. [PubMed: 12888801]
24. Benes FM. Amygdalocortical circuitry in schizophrenia: from circuits to molecules. Neuropsychopharmacology. 2010 Jan; 35(1):239–257. [PubMed: 19727065]
25. Olbrich HG, Braak H. Ratio of pyramidal cells versus non-pyramidal cells in sector CA1 of the human Ammon's horn. Anat Embryol (Berl). 1985; 173(1):105–110. [PubMed: 4073527]
26. Freund TF, Buzsaki G. Interneurons of the hippocampus. Hippocampus. 1996; 6:347–470. [PubMed: 8915675]
27. Klausberger T, Somogyi P. Neuronal diversity and temporal dynamics: the unity of hippocampal circuit operations. Science. 2008 Jul 4; 321(5885):53–57. [PubMed: 18599766]
28. Mann EO, Paulsen O. Role of GABAergic inhibition in hippocampal network oscillations. Trends Neurosci. 2007 Jul; 30(7):343–349. [PubMed: 17532059]
29. Buzsaki, G. Rhythms of the Brain. New York: Oxford University Press; 2006.
30. Bonifazi P, Goldin M, Picardo MA, et al. GABAergic hub neurons orchestrate synchrony in developing hippocampal networks. Science. 2009 Dec 4; 326(5958):1419–1424. [PubMed: 19965761]
31. McBain CJ, Fisahn A. Interneurons unbound. Nat Rev Neurosci. 2001 Jan; 2(1):11–23. [PubMed: 11253355]
32. Viollet C, Lepousez G, Loudes C, Videau C, Simon A, Epelbaum J. Somatostatinergic systems in brain: networks and functions. Mol Cell Endocrinol. 2008 May 14; 286(1–2):75–87. [PubMed: 17997029]
33. Binaschi A, Bregola G, Simonato M. On the role of somatostatin in seizure control: clues from the hippocampus. Rev Neurosci. 2003; 14(3):285–301. [PubMed: 14513869]
34. Bartos M, Vida I, Jonas P. Synaptic mechanisms of synchronized gamma oscillations in inhibitory interneuron networks. Nat Rev Neurosci. 2007 Jan; 8(1):45–56. [PubMed: 17180162]
35. Lewis DA, Hashimoto T, Volk DW. Cortical inhibitory neurons and schizophrenia. Nat Rev Neurosci. 2005 Apr; 6(4):312–324. [PubMed: 15803162]
36. Pantazopoulos H, Lange N, Baldessarini RJ, Berretta S. Parvalbumin neurons in the entorhinal cortex of subjects diagnosed with bipolar disorder or schizophrenia. Biol Psychiatry. 2007 Mar 1; 61(5):640–652. [PubMed: 16950219]
37. Dorph-Petersen KA, Nyengaard JR, Gundersen HJ. Tissue shrinkage and unbiased stereological estimation of particle number and size. J Microsc. 2001 Dec; 204(Pt 3):232–246. [PubMed: 11903800]
38. Gundersen HJ. Stereology of arbitrary particles. A review of unbiased number and size estimators and the presentation of some new ones, in memory of William R. Thompson. J Microsc. 1986 Jul; 143(Pt 1):3–45. [PubMed: 3761363]
39. West MJ, Slomianka L, Gundersen HJ. Unbiased stereological estimation of the total number of neurons in thesubdivisions of the rat hippocampus using the optical fractionator. Anat Rec. 1991 Dec; 231(4):482–497. [PubMed: 1793176]

40. Gundersen HJ, Jensen EB. The efficiency of systematic sampling in stereology and its prediction. J Microsc. 1987 Sep; 147(Pt 3):229–263. [PubMed: 3430576]
41. Gundersen HJ. The nucleator. J Microsc. 1988 Jul; 151(Pt 1):3–21. [PubMed: 3193456]
42. Gundersen HJ, Bagger P, Bendtsen TF, et al. The new stereological tools: disector, fractionator, nucleator and point sampled intercepts and their use in pathological research and diagnosis. APMIS. 1988 Oct; 96(10):857–881. [PubMed: 3056461]
43. Heckers, S. Hippocampus. In: Javitt, D.; Kantrowitz, J., editors. Handboook of Neurochemistry and Molecular Biology, 3rd. edition. Schizophrenia. Vol. Vol 315–330. Berlin: Springer; 2009.
44. Kempton MJ, Geddes JR, Ettinger U, Williams SC, Grasby PM. Meta-analysis, database, and meta-regression of 98 structural imaging studies in bipolar disorder. Arch Gen Psychiatry. 2008 Sep; 65(9):1017–1032. [PubMed: 18762588]
45. Arnone D, Cavanagh J, Gerber D, Lawrie SM, Ebmeier KP, McIntosh AM. Magnetic resonance imaging studies in bipolar disorder and schizophrenia: meta-analysis. Br J Psychiatry. 2009 Sep; 195(3):194–201. [PubMed: 19721106]
46. Amaral, D.; Lavenex, P. Hippocampal neuroanatomy. In: Andersen, P.; Morris, R.; Amaral, D.; Bliss, T.; O'Keefe, J., editors. The hippocampus book. Oxford: Oxford University Press; 2007. p. 37-114.
47. Yushkevich PA, Avants BB, Pluta J, et al. A high-resolution computational atlas of the human hippocampus from postmortem magnetic resonance imaging at 9.4 T. Neuroimage. 2009 Jan 15; 44(2):385–398. [PubMed: 18840532]
48. Boretius S, Kasper L, Tammer R, Michaelis T, Frahm J. MRI of cellular layers in mouse brain in vivo. Neuroimage. 2009 Oct 1; 47(4):1252–1260. [PubMed: 19520174]
49. Ekstrom AD, Bazih AJ, Suthana NA, et al. Advances in high-resolution imaging and computational unfolding of the human hippocampus. Neuroimage. 2009 Aug 1; 47(1):42–49. [PubMed: 19303448]
50. Hanamiya M, Korogi Y, Kakeda S, et al. Partial loss of hippocampal striation in medial temporal lobe epilepsy: pilot evaluation with high-spatial-resolution T2-weighted MR imaging at 3.0 T. Radiology. 2009 Jun; 251(3):873–881. [PubMed: 19346512]
51. Lisman JE. Relating hippocampal circuitry to function: recall of memory sequences by reciprocal dentate-CA3 interactions. Neuron. 1999 Feb; 22(2):233–242. [PubMed: 10069330]
52. Buzsaki G, Chrobak JJ. Temporal structure in spatially organized neuronal ensembles: a role for interneuronal networks. Curr Opin Neurobiol. 1995 Aug; 5(4):504–510. [PubMed: 7488853]
53. Buzsaki G. Hippocampal GABAergic interneurons: a physiological perspective. Neurochem Res. 2001 Sep; 26(8–9):899–905. [PubMed: 11699941]
54. Spencer KM, Nestor PG, Niznikiewicz MA, Salisbury DF, Shenton ME, McCarley RW. Abnormal neural synchrony in schizophrenia. J Neurosci. 2003 Aug 13; 23(19):7407–7411. [PubMed: 12917376]
55. Gonzalez-Burgos G, Lewis DA. GABA neurons and the mechanisms of network oscillations: implications for understanding cortical dysfunction in schizophrenia. Schizophr Bull. 2008 Sep; 34(5):944–961. [PubMed: 18586694]
56. Uhlhaas PJ, Haenschel C, Nikolic D, Singer W. The role of oscillations and synchrony in cortical networks and their putative relevance for the pathophysiology of schizophrenia. Schizophr Bull. 2008 Sep; 34(5):927–943. [PubMed: 18562344]
57. Sanacora G, Rothman DL, Mason G, Krystal JH. Clinical studies implementing glutamate neurotransmission in mood disorders. Ann N Y Acad Sci. 2003 Nov.1003:292–308. [PubMed: 14684453]
58. Frye MA, Tsai GE, Huggins T, Coyle JT, Post RM. Low cerebrospinal fluid glutamate and glycine in refractory affective disorder. Biol Psychiatry. 2007 Jan 15; 61(2):162–166. [PubMed: 16735030]
59. Singh V, Muzina DJ, Calabrese JR. Anticonvulsants in bipolar disorder. Psychiatr Clin North Am. 2005 Jun; 28(2):301–323. [PubMed: 15826734]
60. Clark RE, Squire LR. Classical conditioning and brain systems: the role of awareness. Science. 1998 Apr 3; 280(5360):77–81. [PubMed: 9525860]
61. Schacter DL. Memory and awareness. Science. 1998 Apr 3; 280(5360):59–60. [PubMed: 9556454]

62. Fanselow MS, Dong HW. Are the dorsal and ventral hippocampus functionally distinct structures? Neuron. 2010 Jan 14; 65(1):7–19. [PubMed: 20152109]
63. McClelland JL, McNaughton BL, O'Reilly RC. Why there are complementary learning systems in the hippocampus and neocortex: insights from the successes and failures of connectionist models of learning and memory. Psychol Rev. 1995 Jul; 102(3):419–457. [PubMed: 7624455]
64. Schacter DL, Addis DR. The cognitive neuroscience of constructive memory: remembering the past and imagining the future. Philos Trans R Soc Lond B Biol Sci. 2007 May 29; 362(1481):773–786. [PubMed: 17395575]
65. Wingo AP, Harvey PD, Baldessarini RJ. Neurocognitive impairment in bipolar disorder patients: functional implications. Bipolar Disord. 2009 Mar; 11(2):113–125. [PubMed: 19267694]
66. Liu L, Schulz SC, Lee S, Reutiman TJ, Fatemi SH. Hippocampal CA1 pyramidal cell size is reduced in bipolar disorder. Cell Mol Neurobiol. 2007 May; 27(3):351–358. [PubMed: 17235693]
67. Duan X, Chang JH, Ge S, et al. Disrupted-In-Schizophrenia 1 regulates integration of newly generated neurons in the adult brain. Cell. 2007 Sep 21; 130(6):1146–1158. [PubMed: 17825401]
68. Krivosheya D, Tapia L, Levinson JN, et al. ErbB4-neuregulin signaling modulates synapse development and dendritic arborization through distinct mechanisms. J Biol Chem. 2008 Nov 21; 283(47):32944–32956. [PubMed: 18819924]
69. Foland LC, Altshuler LL, Sugar CA, et al. Increased volume of the amygdala and hippocampus in bipolar patients treated with lithium. Neuroreport. 2008 Jan 22; 19(2):221–224. [PubMed: 18185112]
70. Yucel K, McKinnon MC, Taylor VH, et al. Bilateral hippocampal volume increases after long-term lithium treatment in patients with bipolar disorder: a longitudinal MRI study. Psychopharmacology (Berl). 2007 Dec; 195(3):357–367. [PubMed: 17705060]
71. Javadapour A, Malhi GS, Ivanovski B, Chen X, Wen W, Sachdev P. Hippocampal volumes in adults with bipolar disorder. J Neuropsychiatry Clin Neurosci. 2010 Winter; 22(1):55–62. [PubMed: 20160210]
72. Pantazopoulos H, Woo TU, Lim MP, Lange N, Berretta S. Extracellular matrix-glial abnormalities in the amygdala and entorhinal cortex of subjects diagnosed with schizophrenia. Arch Gen Psychiatry. 2010 Feb; 67(2):155–166. [PubMed: 20124115]
73. Lavenex P, Lavenex PB, Bennett JL, Amaral DG. Postmortem changes in the neuroanatomical characteristics of the primate brain: hippocampal formation. J Comp Neurol. 2009 Jan 1; 512(1): 27–51. [PubMed: 18972553]
74. Chan-Palay V. Somatostatin immunoreactive neurons in the human hippocampus and cortex shown by immunogold/silver intensification on vibratome sections: coexistence with neuropeptide Y neurons, and effects in Alzheimer-type dementia. J Comp Neurol. 1987 Jun 8; 260(2):201–223. [PubMed: 2886516]
75. Schulze TG, Ohlraun S, Czerski PM, et al. Genotype-phenotype studies in bipolar disorder showing association between the DAOA/G30 locus and persecutory delusions: a first step toward a molecular genetic classification of psychiatric phenotypes. Am J Psychiatry. 2005 Nov; 162(11): 2101–2108. [PubMed: 16263850]
76. Lisman JE, Coyle JT, Green RW, et al. Circuit-based framework for understanding neurotransmitter and risk gene interactions in schizophrenia. Trends Neurosci. 2008 May; 31(5): 234–242. [PubMed: 18395805]
77. Heckers S. Making progress in schizophrenia research. Schizophr Bull. 2008 Jul; 34(4):591–594. [PubMed: 18492660]
78. Rogawski MA, Loscher W. The neurobiology of antiepileptic drugs for the treatment of nonepileptic conditions. Nat Med. 2004 Jul; 10(7):685–692. [PubMed: 15229516]

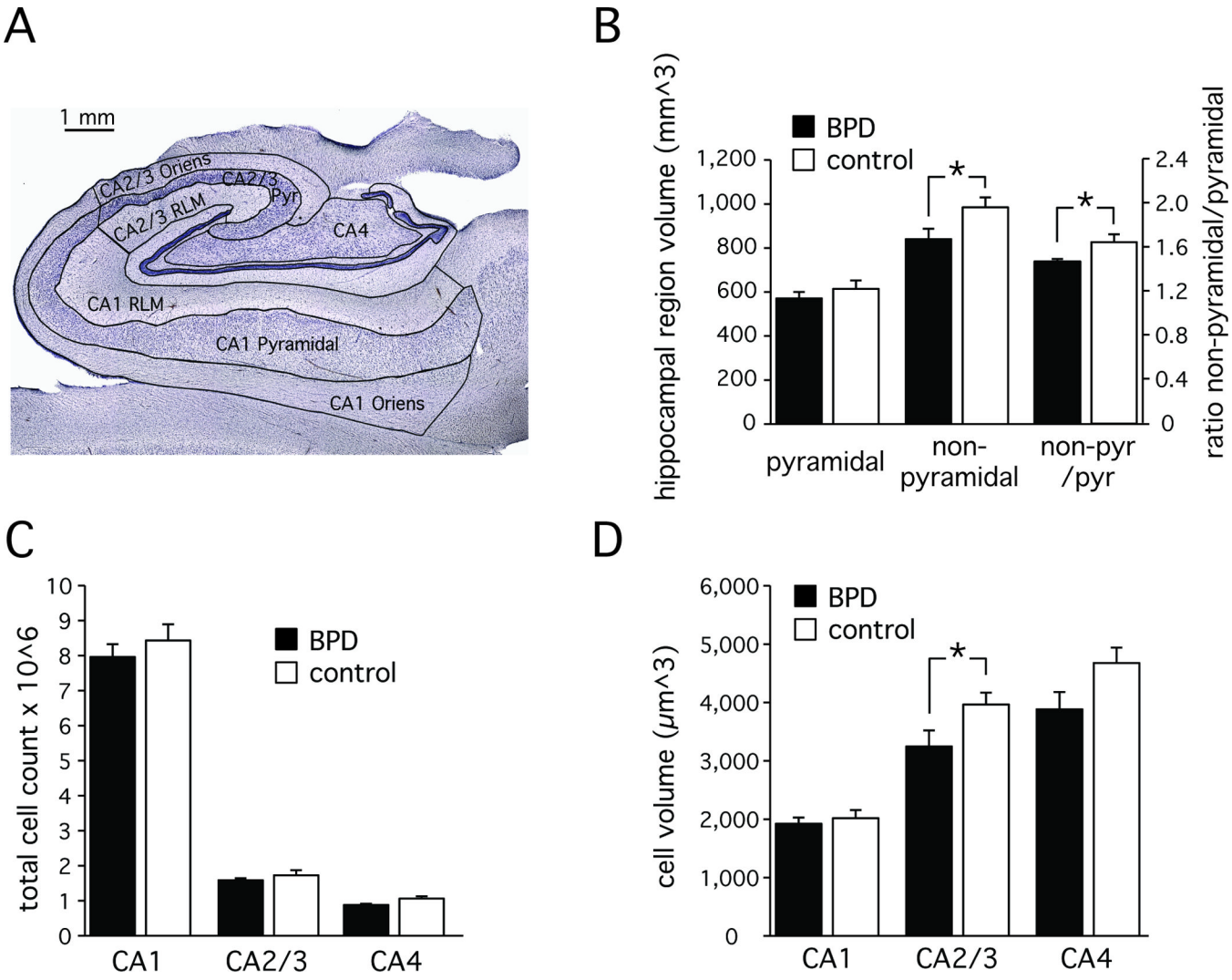

Figure 1. Hippocampal anatomy and cellular organization

A: Coronal section through the body of the hippocampus. The CA1 and CA2/3 sectors have three layers: stratum oriens, stratum pyramidale, stratum radiatum/lacunosum/moleculare (RLM). The CA4 sector has stratum pyramidale only.

B: Ratio of pyramidal and non-pyramidal cell layer volumes in control and bipolar subjects. Non-pyramidal cell layers are reduced in bipolar disorder.

C: Similar cell numbers in the pyramidal cell layer in the CA 1–4 sectors of control and bipolar disorder subjects.

D: Average neuronal cell volume in the CA 1–4 sectors of control and bipolar disorder subjects. Reduction in cell volume in CA2/3.

Average ± SD ; * p<=0.05

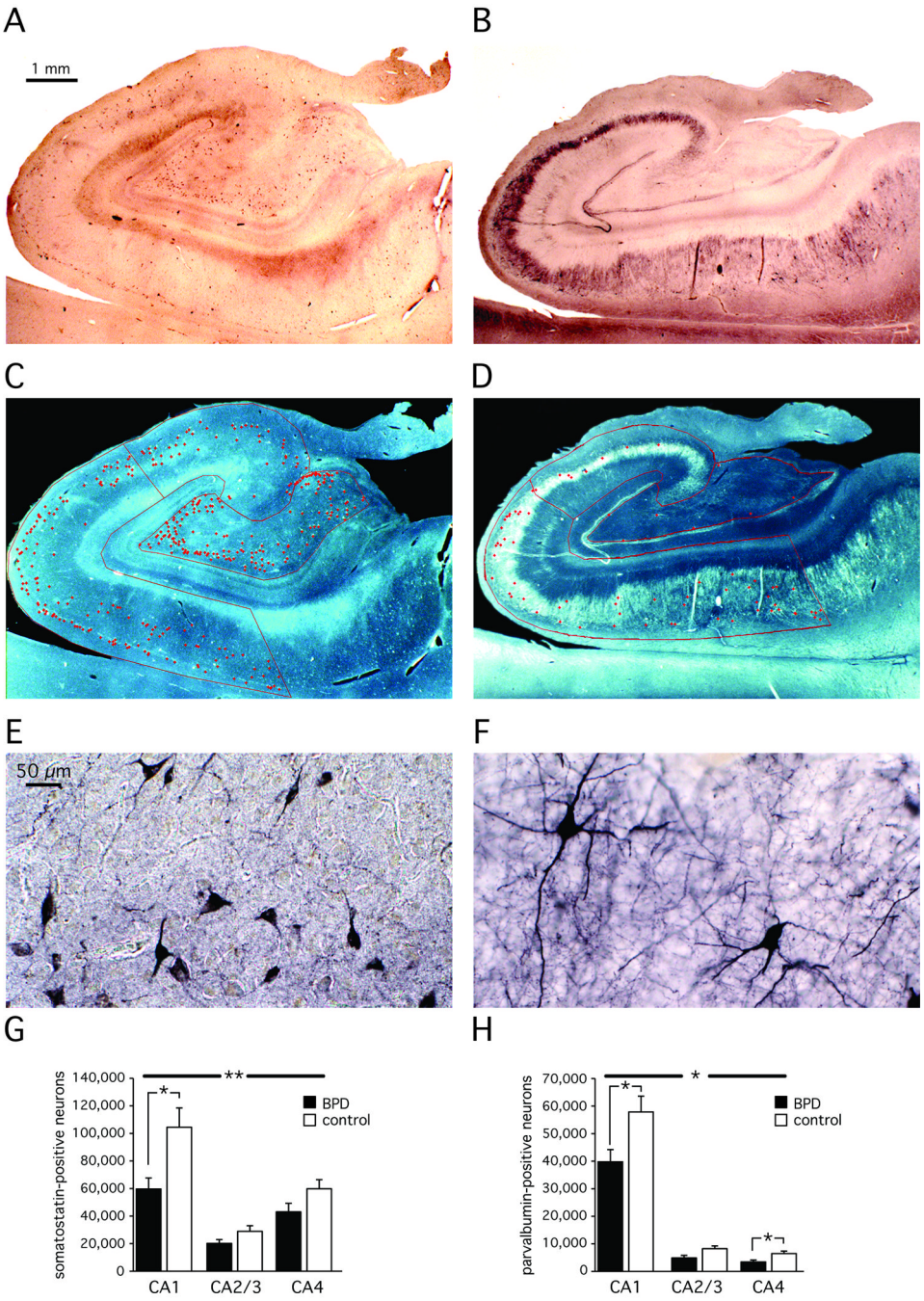

Figure 2. Somatostatin-positive and parvalbumin-positive hippocampal interneurons

An overall reduction of somatostatin-positive (A, C, E, G) and parvalbumin-positive (B, D, F, H) neurons was observed in all sectors of the hippocampus. Post-hoc analysis revealed the sectors with the most significant changes. A, B: representative control case showing immunohistochemical stain; C, D: Overlay of counted cells and hippocampal sectors onto stained tissue; E, F: individually stained cells; G, H: Bar graphs and statistics of all 14 bipolar disorder and 18 control cases.

Average ± SD; * p<=0.05; ** p<=0.01

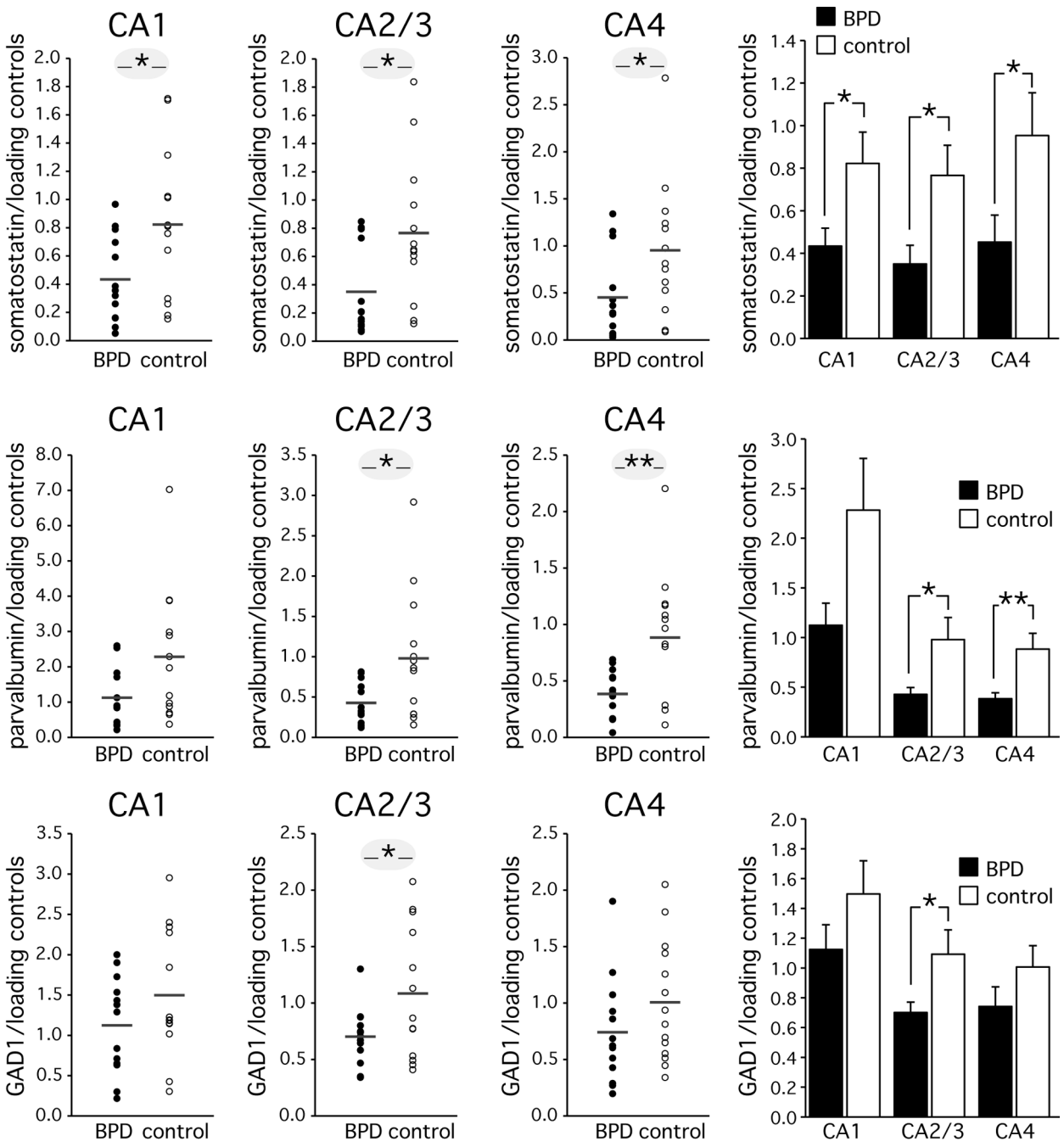

Figure 3. Real-time quantitative PCR analysis of somatostatin, parvalbumin and GAD1 in the hippocampus

Real-time quantitative PCR showed a reduction of somatostatin mRNA levels in all CA sectors. A reduction of parvalbumin mRNA was observed in sectors CA2/3 and CA4. GAD1 mRNA levels were reduced in sector CA2/3. Distribution and bar graphs of 14 bipolar disorder and 14 control cases. All data were normalized to β-actin and filamin A, averaged. Average ± SD; * p<=0.05; ** p<=0.01

Table 1

Demographics of all study subjects

Bipolar Disorder (BPD) subjects were diagnosed according to DSM-IV criteria. For 13 subjects, sufficient information was available to subtype a) BPD type 1 / 2 and b) BPD +/− psychosis. For 11 subjects, information was available to diagnose a family history of non-psychotic mood disorder (n=2), affective psychosis (n=6), psychosis (n=2) or no psychiatric disorder (n=1). n/a - not available.

Group	Case *	Age (years)	Gender	Hemi-sphere	PMI hours)	Cause of death	DSM-IV diagnosis	Age of onset	Duration of illness	Family history	Psychotropic medication
BPD	1	18	M	R	17.9	Motor vehicle accident	n/a	17	1	n/a	Bupropion
BPD	2	23	F	L	24.2	Suicide	BPD 1 +P	16	7	Affective psychosis	Risperidone
BPD	3	38	M	L	22	Suicide (CO poisoning)	BPD 1	17	21	Psychosis	Lorazepam
BPD	4	40	F	R	21.9	Sepsis	BPD 1 +P	22	18	Affective psychosis	-
BPD	5	40	M	L	30.8	Suicide (Hanging)	BPD 1 +P	17	23	Mood disorder	Buspirone, Ziprasidone
BPD	6	47	F	L	16.3	Major systems failure	BPD 1 +P	18	29	Psychosis	Divalproex
BPD	7	51	F	L	35.1	Ischemic heart disease	BPD 1 +P	33	18	None	Clozapine, Venlafaxine
BPD	8	52	F	L	17.2	Liver failure	BPD 1 +P	26	26	Affective psychosis	Lithium
BPD	9	62	F	L	13.4	Congestive heart failure	BPD 1	n/a	n/a	n/a	-
BPD	10	70	M	L	17.3	Renal failure	BPD 1 +P	27	43	Affective psychosis	Lithium
BPD	11	77	F	R	33.3	Pneumonia	BPD 1 +P	n/a	n/a	n/a	Olanzapine, Clomipramine
BPD	12	78	F	R	24.8	Dehydration	BPD 1 +P	28	50	Mood disorder	Lithium
BPD	13	79	F	L	22.6	Ovarian cancer	BPD 1 +P	28	51	Affective psychosis	Trazodone, Carbamazepine, Gabapentine
BPD	14	83	M	R	32.9	Congestive heart failure	BPD 1 +P	29	54	Affective psychosis	Olanzapine, Divalproex, Mirtazapine
Control	1	22	M	R	21.5	Myocardial infarct					
Control	2	36	F	R	18.1	Cardiac arrest					
Control	3	35	M	L	25.7	Myocardial infarct					
Control	4	42	F	L	20.3	Myocardial infarct					
Control	5	41	M	R	27.2	Cardiac arrest					
Control	6	51	F	R	23.1	Cardiac arrest					
Control	7	55	F	R	27.5	Cardiopulmonary arrest					
Control	8	58	F	L	21.1	Myocardial infarct					
Control	9	60	F	L	12.5	Breast cancer					
Control	10	68	M	L	18.4	Heart failure					

Group	Case *	Age (years)	Gender	Hemi-sphere	PMI hours)	Cause of death	DSM-IV diagnosis	Age of onset	Duration of illness	Family history	Psychotropic medication
Control	11	68	F	R	23.9	Cardiopulmonary arrest					
Control	12	74	F	L	23	Pneumonia					
Control	13	81	F	R	17.4	Colon cancer					
Control	14	77	M	L	24.6	Cardiac arrest					
Control	15	52	M	L	13.1	Heart disease					
Control	16	60	F	R	17.8	Cardiac dysrythmia					
Control	17	60	M	L	30.3	Cardiac arrest					
Control	18	86	F	L	6.9	Cardiac arrest					
BPD	**14**	**54.1 ± 21.2**	**9F / 5M**	**9L / 5R**	**23.5 ± 7.0**						
Control 1	**14**	**54.9 ± 17.8**	**9F / 5M**	**7L / 7R**	**21.7 ± 4.2**						
Control 2	**18**	**57.0 ± 17.3**	**11F / 7M**	**10L / 8R**	**20.7 ± 5.9**						

* Cases 1–14 in each group were matched pair-wise for age and gender. These pairs were used for the Q-PCR experiment.